Proceedings of Workshop on Applications of Synchrot
Light to Magnetic Materials, Campinas, Brazil
August 14-16, 2000 (to be published in JMMM)

BNL-67705

X-ray Resonant Scattering Studies of Charge and Orbital Ordering in $Pr_{1-x}Ca_xMnO_3$

M. v. Zimmermann[1], C.S. Nelson[1], J. P. Hill[1], Doon Gibbs[1],
M. Blume[1], D. Casa[2], B. Keimer[2], Y. Murakami[3], C.-C. Kao[4],
C. Venkataraman[5], T. Gog[5] Y. Tomioka[6] and Y. Tokura[7]

[1] *Department of Physics, Brookhaven National Laboratory Upton, NY 11973-5000*

[2] *Department of Physics, Princeton University Princeton, NJ 08544 and Max-Planck-Institut fur Festoperforschung 70569 Stuttgart, Germany*

[3] *Photon Factory, Institute of Materials Structure Science High Energy Accelerator Research Organization Tsukuba 305-0801, Japan*

[4] *National Synchrotron Light Source, Brookhaven National Laboratory Upton, NY 11973-5000*

[5] *CMC-CAT, Advanced Photon Source, Argonne National Laboratory Argonne, IL 60439*

[6] *Joint Research Center for Atom Technology (JRCAT) Tsukuba 305-0033, Japan*

[7] *Department of Applied Physics, University of Tokyo Tokyo 113-0033, Japan*

We present the results of x-ray scattering studies of the charge and orbital ordering in the manganite series $Pr_{1-x}Ca_xMnO_3$ with x=0.25, 0.4 and 0.5. The polarization and azimuthal dependence of the charge and orbital ordering in these compounds is characterized both in the resonant and nonresonant limits, and compared with the predictions of current theories. The results are qualitatively consistent with both cluster and LDA+U calculations of the electronic structure.

Interest in the origins of high temperature superconductivity and colossal magnetoresistance in the transition metal oxides has driven much of the activity currently at the center of condensed matter physics. An important aspect of these strongly correlated electron systems is that no single degree of freedom dominates their response. Rather, the ground state properties are thought to reflect a balance among several correlated processes, including orbital and charge ordering, magnetism, and coupling to the lattice.

The perovskite manganites provide an especially illuminating example of the interplay among these interactions, since in these materials the balance may be conveniently altered, for example by doping or through an applied magnetic field. As a result, much work has been done to understand their magnetic ground states and lattice distortions, dating back to the seminal experiments of Wollan and Koehler [1]. Less is known about the roles of charge and orbital order in these materials. The classic work of Goodenough [2] has nevertheless served as a guide to their ordered arrangements, as supplemented, for example, by detailed measurements of the crystal structure and of the temperature dependence of the lattice constants (see references [3,4], for example).

This situation has changed during the last two years following the detection of orbital and charge order by resonant x-ray scattering techniques [5–11]. Specifically, it has been found that the sensitivity of x-ray scattering to these structures can be significantly enhanced by tuning the incident x-ray energy to the transition metal K-absorption edge. Thus, it appears possible to characterize the orbital and charge ordering on a microscopic scale, and to study their response to changes of temperature or to an applied magnetic field. Insofar as we are aware, resonant x-ray scattering studies of these materials have now been extended to include $La_{0.5}Sr_{1.5}MnO_4$ [5], $LaMnO_3$ [6], $La_xSr_{1-x}MnO_3$ [10,12], $Pr_{1-x}Ca_xMnO_3$ [13], V_2O_3 [14], $YTiO_3$ [15], $LaTiO_3$ [16], $LaSr_2Mn_2O_7$ [17], DyB_2C_2 [18,19], and $Nd_{0.5}Sr_{0.5}MnO_3$ [20,21],–and this list continues to grow. There is, in addition, an ongoing discussion of whether it is more appropriate to treat the resonant cross-section within an extended, band structure description of the electronic structure, or instead with a more localized, atomic description [9,22,7,11]. A related question concerns how to write the resonant cross-section

explicitly in terms of the order parameters for orbital and charge ordering.

In this paper, we summarize x-ray scattering studies of $Pr_{1-x}Ca_xMnO_3$ with x=0.25, 0.4 and 0.5. Detailed measurements of the polarization and azimuthal dependence of the charge and orbital ordering have been carried out in both the resonant and nonresonant limits. In the $\sigma \rightarrow \pi$ channel at the orbital wavevector of all three samples, we find that the resonant cross-section is qualitatively consistent with the results obtained earlier for $LaMnO_3$ [6] and with the predictions of both the localized and band-structure descriptions of the electronic structure. Likewise, we have found that the resonant scattering at the charge order wavevector is consistent with earlier results obtained for $La_{1.5}Sr_{0.5}MnO_4$ [5]. We have, in addition, discovered scattering in the $\sigma \rightarrow \sigma$ channel at the charge and orbital wavevectors of the x=0.4 and 0.5 samples. On the basis of its polarization and Q-dependence, we have deduced that it originates from a longitudinal lattice modulation. Earlier studies of $La_{0.5}Ca_{0.5}MnO_3$, had previously found a transverse modulation [4,23–25], and a similar modulation has been assumed in $Pr_{1-x}Ca_xMnO_3$. A more detailed version of the present work has been discussed elsewhere [13].

At room temperature, the crystal structure of $Pr_{1-x}Ca_xMnO_3$ is orthorhombic (Pbmn). Characteristic of the perovskite manganites, each Mn atom lies at the center of the octahedron defined by the oxygen atoms at the corners. Single layers of Pr atoms lie between the layers of octahedra. Depending on the temperature, there may be distortions of the octahedra, as well as tilts.

For small x ($0.15 \leq x \leq 0.3$) and at low temperatures, $Pr_{1-x}Ca_xMnO_3$ is a ferromagnetic insulator, and is believed to exhibit an orbitally ordered ground state analogous to that observed in $LaMnO_3$ [26,27]. The electronic configuration of the Mn^{3+} (d^4) ions is (t_{2g}^3, e_g^1) with the t_{2g} electrons localized at the Mn sites. The e_g electrons are hybridized with the oxygen 2p orbitals, and believed to participate in a cooperative Jahn-Teller distortion of the MnO_6 octahedra. This leads to a $(3x^2 - r^2)$-$(3y^2 - r^2)$-type of orbital order of the e_g electrons in the ab plane with the oxygens displaced along the direction of extension of the e_g orbitals. A schematic illustration of this orbitally ordered state for x=0.25 is shown in

Figure 1a [3], with the orbital unit cell marked by the solid line. The excess Mn^{4+} ions in this material are believed to be disordered. It is noteworthy that the orbital period is twice that of the fundamental Mn spacing, so that orbital scattering appears at structurally forbidden reflections. In orthorhombic notation, for which the fundamental Bragg peaks occur at (0,2k,0), the orbital scattering then occurs at (0,k,0).

For Ca concentrations $0.3 \leq x \leq 0.7$, $Pr_{1-x}Ca_xMnO_3$ becomes an antiferromagnetic insulator at low temperatures, and exhibits colossal magnetoresistance in applied magnetic fields, with the metal-insulator transition occurring between 5 and 8 T [28]. These effects result from charge ordering among the Mn^{3+} and Mn^{4+} ions, which occurs in addition to orbital ordering. The large conductivity is enabled through the hopping of e_g electrons among Mn sites. The fraction of Mn ions in the Mn^{4+} state is determined largely by the concentration of Ca ions. Thus, by varying the Ca concentration, it is possible to alter the balance between charge and orbital ordering. The proposed ground state [3] for both the x=0.4 and x=0.5 concentrations is shown in Figure 1b. The small filled circles represent the Mn^{4+} ions, with one fewer electron than is localized at the Mn^{3+} sites. The solid line indicates the unit cell for orbital ordering, while the dashed line gives that for charge ordering. Note that the orbital period in the x=0.4, 0.5 compounds differs from that occurring in samples with x<0.3, as a result of the presence of charge ordering.

The magnetic structure of these compounds at low doping ($0.15 \leq x \leq 0.3$) is ferromagnetic with $T_C \approx 140$ K. Compounds with higher doping ($0.3 \leq x \leq 0.75$) are CE-type antiferromagnets with T_N=170 K for x between 0.4 and 0.5 [3]. The in-plane components of the magnetic structures are also illustrated in Figure 3.

Figure 2 shows the energy dependence of the scattering at the (100) orbital wavevector of the x=0.25 sample as the incident x-ray energy is tuned through the Mn K absorption edge (6.539 keV). These data were obtained with a Si(111) analyzer on the CMC-CAT undulator beamline 9ID at the APS. A large resonant signal is visible at $\hbar\omega$=6.547 keV, reaching more than 20,000 counts per second near the edge. In addition, there are two smaller peaks at higher energies ($\hbar\omega$=6.56 and 6.575 keV), and one below (at $\hbar\omega$=6.534 keV). The inset shows

the lower energy peak in more detail. No signal was observed at energies 100 eV above or below the absorption edge, implying that only pure resonant scattering was present in this sample. Polarization analysis suggests that the scattered signal is predominantly π polarized, consistent with a rotation of the incident linear polarization from being perpendicular to the diffraction plane, σ, to lying within the diffraction plane, π. It should be added that all of the data shown here were obtained at an azimuthal angle $\psi = 90°$. As a function of azimuthal angle, the resonant intensity observed for the x=0.25 sample takes maxima at ψ=90 and 270°, and minima at 0 and 180°. These results are all similar to those obtained previously at the orbital wavevector of $LaMnO_3$, including the 4-peaked fine structure in the energy dependence, an identical polarization and azimuthal dependence, and the absence of nonresonant scattering away from the edge [5,29].

Figures 3a and 3b show the energy dependence of the scattering at the (0,1.5,0) and (0,2.5,0) orbital wavevectors of the x=0.4 sample, again as the incident x-ray energy is tuned through the Mn K absorption edge. These data were obtained on the X22C bending magnet beamline at the NSLS, and explicitly resolve the polarization. The closed circles show the $\sigma \rightarrow \pi$ scattering, and the open circles show the $\sigma \rightarrow \sigma$ scattering. Although the fine structure in figure 2a is not as clearly resolved as in the x=0.25 sample, the main features of the $\sigma \rightarrow \pi$ scattering are similar, including a pronounced resonance peak at 6.547 keV and a weaker peak at 6.56 keV. In contrast to the $\sigma \rightarrow \pi$ scattering, the $\sigma \rightarrow \sigma$ scattering shows a double peaked structure with a pronounced dip at the absorption edge. This is strongly reminiscent of the behavior of charge scattering, and suggests the presence of a lattice modulation with the orbital wavevector. The fact that the $\sigma \rightarrow \sigma$ intensity does not fall off at lower x-ray energy, but instead continues above background, is further evidence of a significant nonresonant signal as would be produced by such a modulation. Lattice modulations associated with the CE type structure have been observed before in $Pr_{1-x}Ca_xMnO_3$ e.g. [3,30,31] and also in $La_{0.5}Ca_{0.5}MnO_3$ [4,19,21]. In the latter compound, the structure was solved, and the modulation found to be purely transverse. Such a modulation, however, is inconsistent with the present results.

To summarize: In all three samples, we find a pure resonant signal in the $\sigma \rightarrow \pi$ channel at the appropriate orbital wavevector with the dominant peak located near the Mn K absorption edge. Additional fine structure is observed both above and below the absorption edge. The π-resonant scattering has the characteristic azimuthal dependence, varying as $\sin^2 \psi$, where ψ is the azimuthal angle. These results are identical to what has been observed previously in $LaMnO_3$ [6] and $La_{0.5}Sr_{1.5}MnO_4$ [5]. In the x=0.4 and 0.5 samples, there is in addition a $\sigma \rightarrow \sigma$ component of the scattering at the orbital wavevector with both resonant and nonresonant parts. The non-resonant component lacks any azimuthal dependence and is consistent with normal charge scattering. The x=0.25 sample lacks a $\sigma \rightarrow \sigma$ component to within the detection limits of the experiment, as was also the case in $LaMnO_3$.

We associate the dominant, resonant peak, which occurs in the $\sigma \rightarrow \pi$ channel of all three samples with the electric dipole transition coupling 1s and 4p states, as discussed in reference 13. In this description, the sensitivity to orbital ordering may be thought of, qualitatively, as arising from a splitting of the Mn 3d states, either through the Jahn-Teller distortion of the oxygen atoms or through a Coulomb interaction. In either case, the existence of a dipole resonance in the $\sigma \rightarrow \pi$ channel, and the observed azimuthal dependence, are consistent with theoretical predictions. We, therefore, interpret the observed resonant scattering as Templeton scattering induced by the orbital ordering, just as previously concluded for $LaMnO_3$ and $La_{0.5}Sr_{1.5}MnO_4$ [5,6]. To explain the additional fine structure both above and below the main peak, however, requires a more sophisticated treatment. Elfimov et al. [9], in particular, have performed band structure calculations for $LaMnO_3$ with a LSDA+U-type approach, and shown that the fine structure above the absorption edge reflects the 4p density of states after hybridization of the central Mn 4p and surrounding O 2p states. They show further that the higher energy peaks originate predominantly from the Jahn-Teller distortion of the oxygens, and not from direct Coulomb interactions. In contrast, the small peak about 13 eV below the white line is associated with the intersite 4p-3d Coulomb interaction of the central and neighboring Mn ions via the intervening O 2p states. Although quantitative comparisons remain to be made, the qualitative agreement

between these predictions and the observed spectra is good, and offers a natural description of the experimental results. In this regard, it should be added that Ishihara *et al.* [32] have also carried out cluster calculations of the resonant cross-section in $LaSr_2Mn_2O_7$, assuming an intra-site 3d-4p Coulomb origin of the 4p splitting. By including band effects, they also were able to produce qualitatively similar fine structure above the Mn K edge. Thus, we are not able to distinguish a possible Coulomb origin of the resonant peak from a Jahn-Teller origin on the basis of our experiments —however, the additional fine structure at higher photon energies appears to result from band effects in both approaches.

We turn next to the lattice modulation observed at the orbital wave-vector in the $\sigma \rightarrow \sigma$ channel. Such modulations have been observed before in CE-type structures, and in particular in $Pr_{1-x}Ca_xMnO_3$ by neutron [3,31] and non-resonant x-ray scattering [31,33]. Similar results have also been obtained in $La_{0.5}Ca_{0.5}MnO_3$ [4] at $(h, \frac{k}{2} - \epsilon, 2n)$, where $h \neq 0$ and ϵ, the incommensurability, is weak (we have converted to P_{bnm} settings to be consistent with the rest of the present paper). The latter structure was solved by x-ray powder diffraction and a purely transverse modulation of the Mn^{4+} sites was deduced, wherein the Mn^{4+} sites are displaced along the a-direction with a periodicity equal to the orbital periodicity. All of the orbital superlattice peaks observed to date in the $Pr_{1-x}Ca_xMnO_3$ system have also had a significant a-axis component and a similar distortion has been assumed [3].

In the present case, the $\sigma \rightarrow \sigma$ scattering observed at $(0, k + \frac{1}{2}, 0)$ requires a longitudinal b-axis component of the modulation. This follows from the small-displacement limit of the x-ray intensity, which varies as $Q \cdot \delta$ to leading order for displacements of the form $\delta \sin(\tau.R)$. For x=0.4 and 0.5, we did not examine reflections of the form (h/2,0,l) with $l \neq 0$ and cannot draw conclusions about displacements in other directions, however, we have recently performed limited studies on an x=0.3 sample in which the orbital reflections around (0,2,0) and (2,2,0) were studied. The non-resonant scattering was observed to be significantly stronger in the vicinity of the (220) consistent with a larger transverse displacement and a small longitudinal modulation [34].

Figures 4a and 4b show the energy dependence of the scattering at the (0,1,0) and (0,3,0)

charge order wavevectors of the x=0.4 sample, as the incident x-ray energy is tuned through the Mn K absorption edge. These data were obtained at the NSLS beamline X22C and are polarization resolved. The open circles show the $\sigma \rightarrow \sigma$ scattering and the closed circles the $\sigma \rightarrow \pi$ scattering. No signal was obtained in the $\sigma \rightarrow \pi$ channel, to within the detection limits of the experiment. In the $\sigma \rightarrow \sigma$ channel the (0,1,0) reflection has a shoulder at lower energy which rises to a resonant peak at 6.538 keV. This is followed by a dip and another smaller peak centered near 6.57 keV. The profile of the (0,3,0) reflection shows a resonant peak at slightly higher energy (6.540 keV) relative to the (0,1,0) reflection, and the additional structure appears inverted. This is a clear signature of an interference process, involving the resonant and nonresonant contributions to the charge order scattering. The nonresonant scattering may, in principle, result from the valence modulation itself (which is weak), or from an accompanying lattice modulation, or both. The resonant scattering arises from the anomalous parts of the Mn^{3+} and Mn^{4+} scattering factors, which are distinct. A more detailed discussion of these results is given in reference 13.

I. CONCLUSIONS

This paper briefly describes charge and orbital ordering studies of the manganate series $Pr_{1-x}Ca_xMnO_3$ with x = 0.25, 0.4 and 0.5. The polarization and azimuthal dependence of the resonant charge and orbital ordering at the K edge is found to be qualitatively consistent with the predictions of a simple model in which the 4p levels are split in the orbitally ordered phase. The experiments do not distinguish among more sophisticated treatments of the electronic structure, whether in atomic or band limits. These results illustrate the kinds of information which can be obtained concerning transition metal oxides using x-ray resonant scattering techniques.

II. ACKNOWLEDGEMENTS

We acknowledge helpful conversations with S. Ishihara, D.J. Khomskii, A. J. Millis, and G. A. Sawatzky. The work at Brookhaven, both in the Physics Department and at the NSLS, was supported by the U.S. Department of Energy, Division of Materials Science, under Contract No. DE-AC02-98CH10886, and at Princeton University by the N.S.F. under Grant No. DMR-9701991. Support from the Ministry of Education, Science and Culture, Japan, by the New Energy and Industrial Technology Development Organization (NEDO), and by the Core Research for Evolution Science and Technology (CREST) is also acknowledged. Work at the CMC beamlines is supported, in part, by the Office of Basic Energy Sciences of the U.S. Department of Energy and by the National Science Foundation, Division of Materials Research. Use of the Advanced Photon Source was supported by the Office of Basic Energy Sciences of the U.S. Department of Energy under Contract No. W-31-109-Eng-38.

REFERENCES

[1] E. Wollan and W. Koehler, Phys. Rev. **100**, 545 (1955).

[2] J. Goodenough, Phys. Rev. **100**, 555 (1955).

[3] Z. Jirak, S. Krupica, Z. Simsa, M. Dlouha and S. Vratislav, J. Magn. Magn. Mat. **53**, 153 (1985).

[4] P.G. Radaelli, D.E. Cox, M. Marezio and S.-W. Cheong, Phys. Rev. B **55**, 3015 (1997).

[5] Y. Murakami, H. Kawada, H. Kawata, M. Tanaka, T. Arima, Y. Moritomo and Y. Tokura, Phys. Rev. Lett. **80**, 1932 (1998).

[6] Y. Murakami, J.P. Hill, D. Gibbs, M. Blume, I. Koyama, M. Tanaka, H. Kawata, T. Arima, Y. Tokura, K. Hirota and Y. Endoh , Phys. Rev. Lett. **81**, 582 (1998).

[7] S. Ishihara and S. Maekawa, Phys. Rev. Lett. **80**, 3799 (1998).

[8] M. Fabrizio, M. Altarelli and M. Benfatto, Phys. Rev. Lett. **80**, 3799 (1998).

[9] I.S. Elfimov, V.I. Anisimov and G.A. Sawatsky, Phys. Rev. Lett. **82**, 4264 (1999).

[10] Y. Endoh, K. Hirota, S. Ishihara, S. Okamoto, Y. Murakami, A. Nishizawa, T. Fukada H. Kimura, H. Nohiri, K. Kaneoko and S. Maekawa, Phys. Rev. Lett. **82**, 4328 (1999).

[11] P. Fulde, J. Phys. Soc. Jpn. **5**, 154 (2000).

[12] P. Wochner *et al.*, Unpublished .

[13] M. v. Zimmermann, J.P. Hill, D. Gibbs, M. Blume, D. Casa, B. Keimer, Y. Murakami, Y. Tomioka and Y. Tokura, Phys. Rev. Lett. **83**, 4872 (1999, and submitted to Phys. Rev. B).

[14] L. Paolosini, C. Vettier, F. de Bergevin, D. Mannix, W. Neubeck, A. Stunault, F. Yakhou, J.M. Honig and P.A. Metcalf, Phys. Rev. Lett. **82**, 4719 (1999).

[15] H. Nakao *et al.*, Unpublished .

[16] B. Keimer, D. Casa, A. Ivanov, J.W. Lynn, M. v. Zimmermann, J.P. Hill, D. Gibbs, Y. Toguchi and Y. Tokura, cond-mat/0002014 .

[17] Y. Wakabayashi, Y. Murakami, I. Koyama, T. Kimura, Y. Tokura, Y. Moritomo, K. Hirota, and Y. Endoh, Preprint (2000).

[18] Y. Tanaka, T. Inami, T. Wakamura, H. Yamauchi, H. Onoderon, K. Ohoyama, and Y. Yamaguchi, J. Phys. Condens. Matter **11**, L505 (1999).

[19] K. Hirota, N. Oumi, T. Matsumura, H. Nakao, Y. Wakabayashi, Y. Murakami, and Y. Endoh, Phys. Rev. Lett. **84**, 2706 (2000).

[20] K. Nakamura, T. Arina, A. Nakazawa, Y. Wakabayashi, and Y. Murakami, Phys. Rev. B **60**, 2425 (2000).

[21] P. Hatton, Bulletin, Stefan University **11**, 337 (1999).

[22] M. Benfatto, Y. Joly, and C.R. Natoli, Phys. Rev. Lett. **83**, 636 (1999).

[23] P.G. Radaelli, D.E. Cox, L. Capogna, S.-W. Cheong and M. Marezio, Phys. Rev. B **59**, 14440 (1999).

[24] R. Wang, J. Gui, Y. Zhu and A. Moodenbaugh, preprint EUR .

[25] C.H. Chen and S.-W. Cheong, Phys. Rev. Lett. **76**, 4042 (1990).

[26] Y. Tokura and Y. Tomioka, J. Magn. Magn. Mater. **200**, 1 (1999).

[27] M. Blume, in *Resonant Anomalous X-ray Scattering* (North-Holland, Amsterdam, 1991), p. 495.

[28] Y. Tomioka, A. Asamitsu, H. Kawahara, Y. Moritomo and Y. Tokura, Phys. Rev. B **53**, 1689 (1996).

[29] Y. Murakami *et al.*, Unpublished .

[30] H. Yoshizawa, H. Kiwano, Y. Tomioka and Y. Tokura, Phys. Rev. B **52**, R13145

(1995).

[31] V. Kiryukhin, D. Casa, J.P. Hill, B. Keimer, A. Vigliante, Y. Tomioka and Y. Tokura, Nature **386**, 813 (1997).

[32] S. Ishihara and S. Maekawa, Phys. Rev. B **62**, xxxx (2000).

[33] D. Cox, P.G. Raedelli, M. Marezio, and S.-W. Cheong, Phys. Rev. B **57**, 3305 (1998).

[34] C.S. Nelson, M. v. Zimmermann, J.P. Hill, D. Gibbs, D. Casa, B. Keimer, T. Gog, and C. Venkataraman, Unpublished work .

FIGURES

FIG. 1. Schematic of the charge, orbital and magnetic order in $Pr_{1-x}Ca_xMnO_3$. Filled circles represent Mn^{4+} ions, shaded figure-eights represent Mn^{3+} ions, and the arrows indicate the in-plane components of the magnetic ordering. Solid lines show orbital order unit cell; dashed lines show the charge order unit cell. (a) Orbital ordering for x=0.25, (b,c) Charge and orbital order for x=0.4 and 0.5., and (c) shows an orbital antiphase domain wall.

FIG. 2. Intensity plotted versus incident photon energy of the orbital (010) reflection of the x=0.25 sample near the Mn white line at 6.555 keV. These data were taken at APS beamline 9ID with an energy resolution of 1.5 eV. Inset: Close-up of the pre-edge feature at 6.535 keV.

FIG. 3. Polarization-resolved scans of intensity plotted versus incident photon energy of the orbital (0,1.5,0) and (0,2.5,0) reflections of the x=0.4 sample near the Mn K-absorption edge.

FIG. 4. Polarization-resolved scans of the intensity plotted versus incident photon energy of the charge (0,1,0) and (0,3,0) reflections of the x=0.4 sample near the Mn K absorption edge.

a)

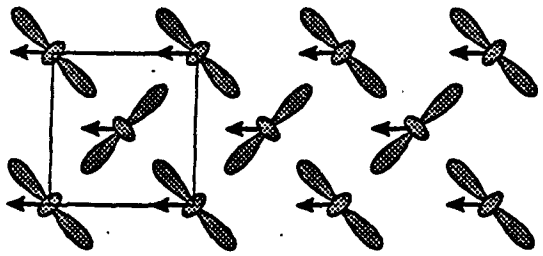

b)

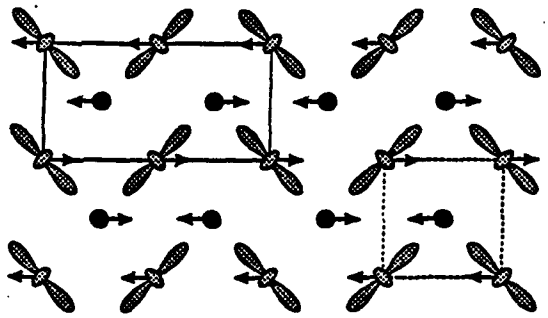

c)

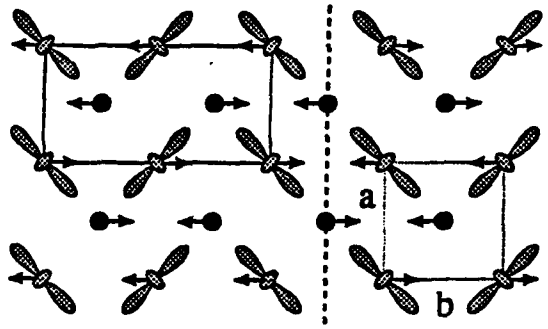

Fig. 1

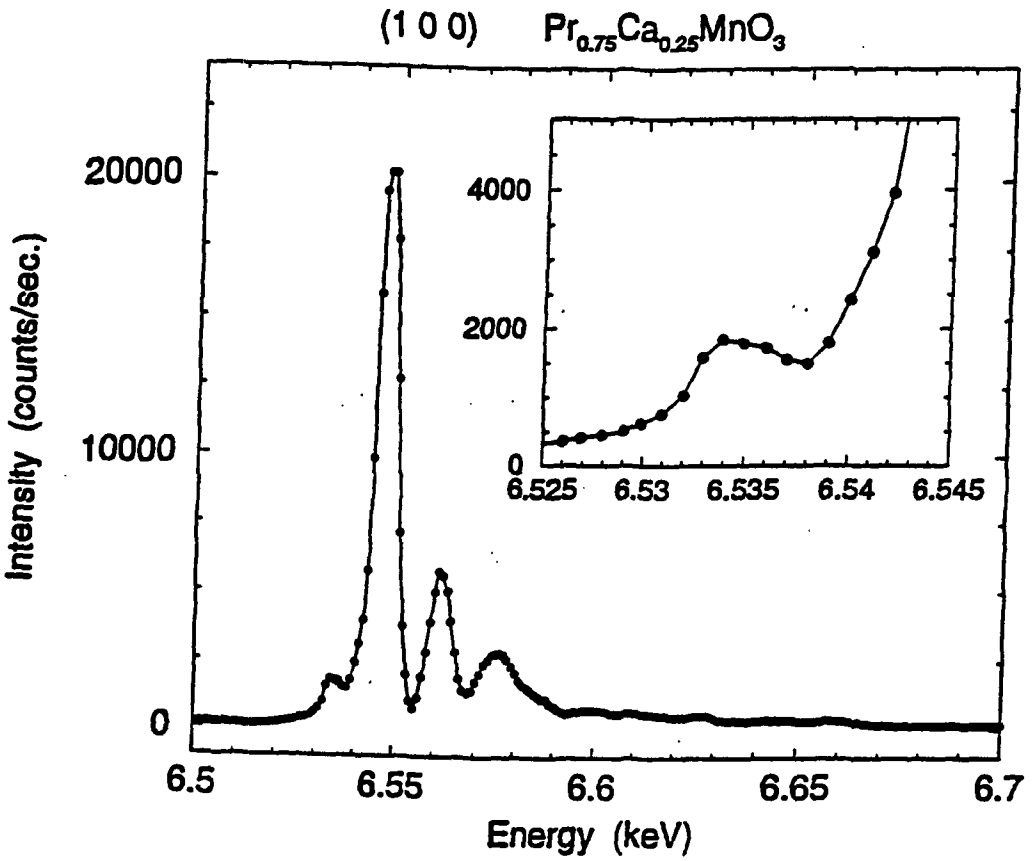
(1 0 0) $Pr_{0.75}Ca_{0.25}MnO_3$
Intensity (counts/sec.)
20000
10000
0
6.5
6.55
6.6
6.65
6.7
Energy (keV)
4000
2000
0
6.525
6.53
6.535
6.54
6.545

Fig 2

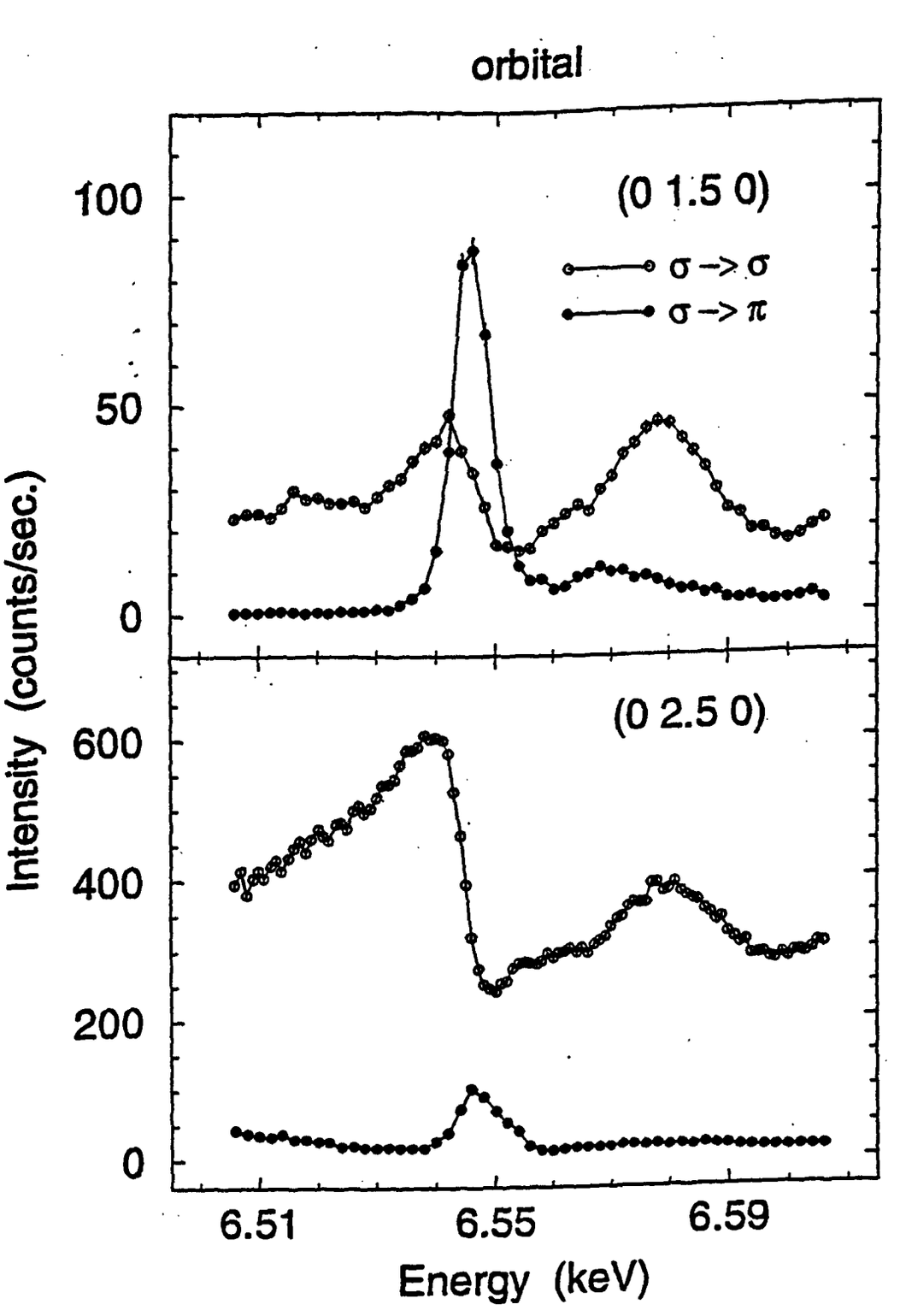
orbital
(0 1.5 0)
σ -> σ
σ -> π
100
50
0
(0 2.5 0)
600
400
200
0
Intensity (counts/sec.)
6.51
6.55
6.59
Energy (keV)

Fig. 3

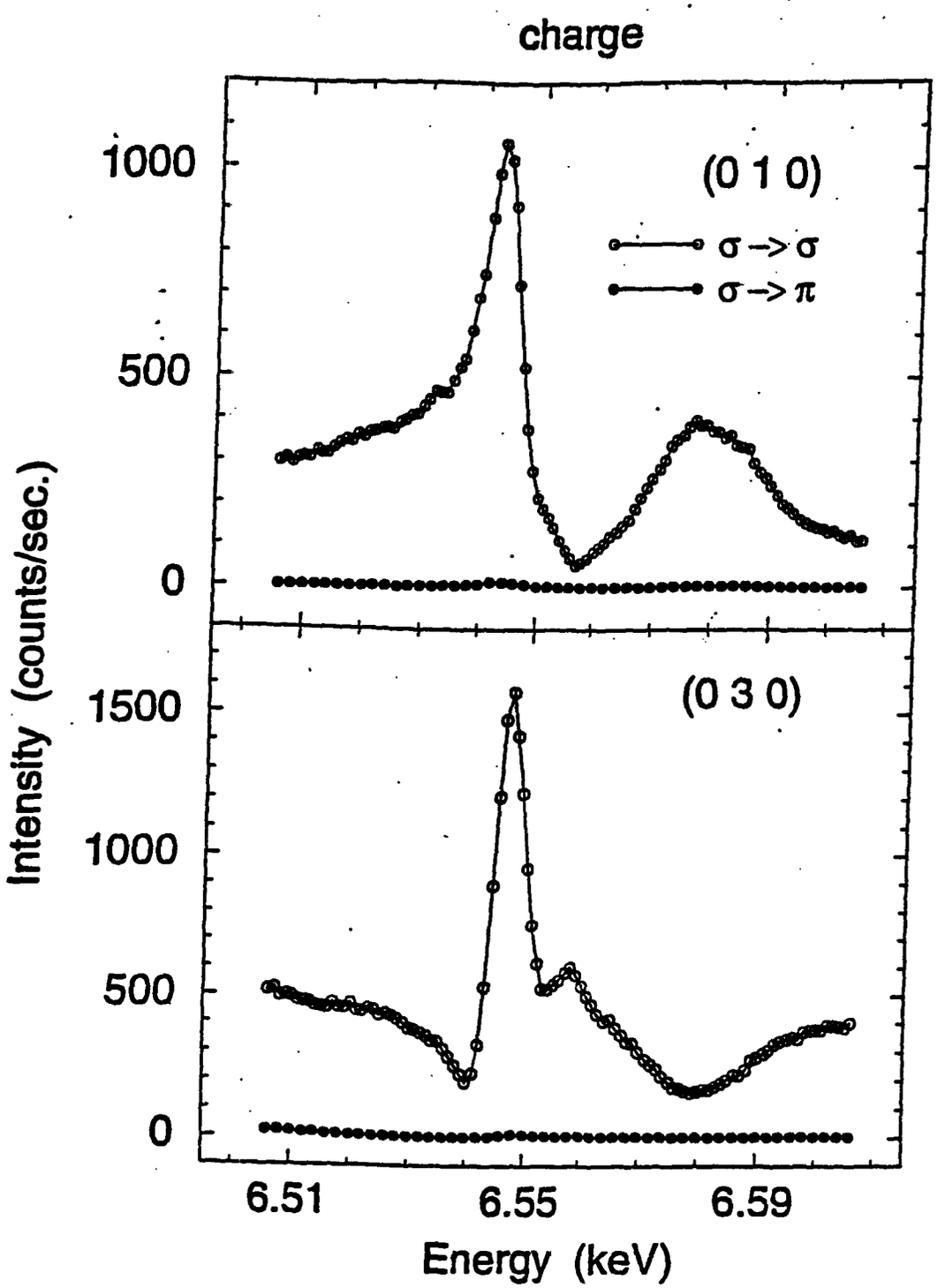
charge
(0 1 0)
σ -> σ
σ -> π
1000
500
0
(0 3 0)
1500
1000
500
0
Intensity (counts/sec.)
6.51
6.55
6.59
Energy (keV)

Fig 11